A model for the decomposition kinetics of the bulk amorphous $Zr_{41}Be_{22.5}Ti_{14}Cu_{12.5}Ni_{10}$ alloy

1997 J. Phys.: Condens. Matter 9 L509

(http://iopscience.iop.org/0953-8984/9/37/003)

J. Phys.: Condens. Matter **9** (1997) L509–L516. Printed in the UK PII: S0953-8984(97)86137-1

LETTER TO THE EDITOR

A model for the decomposition kinetics of the bulk amorphous $Zr_{41}Be_{22.5}Ti_{14}Cu_{12.5}Ni_{10}$ alloy

Helmut Hermann†, Albrecht Wiedenmann‡ and Patric Uebele†

† Institute of Solid State and Materials Research Dresden, Postfach 270016, D-01171 Dresden, Germany

‡ Hahn-Meitner Institute Berlin, Glienicker Strasse 100, D-14109 Berlin, Germany

Received 16 July 1997

Abstract. Recent experimental data on decomposition phenomena of bulk amorphous $Zr_{41}Be_{22.5}Ti_{14}Cu_{12.5}Ni_{10}$ alloy in the supercooled liquid state are explained in terms of a theoretical model. The model includes two different aspects: (i) nucleation and diffusion limited growth of (amorphous) spherical precipitates and (ii) ordering effects due to hardcore-like interaction of the diffusion zones around the precipitates. For the early stages of decomposition and low volume fraction of precipitates the model is treated analytically whereas for medium and high volume fraction computer simulation is necessary. The theoretical results are compared to experimental small-angle neutron scattering curves obtained for different annealing times and temperatures. The comparison shows that the proposed model is suitable to describe the decomposition of the alloy during annealing within the supercooled liquid state.

The $Zr_{41}Be_{22.5}Ti_{14}Cu_{12.5}Ni_{10}$ alloy belongs to a new class of amorphous materials. It can be prepared from the liquid phase at very low cooling rates as large bulky ingots [1–3]. The supercooled liquid state of the alloy is preserved in a wide temperature range between the glass temperature, $T_g = 622$ K, and $T_{x_1} = 673$ K where crystallization occurs. Thermal stability and decomposition phenomena in the supercooled temperature regime, $T_g < T < T_{x_1}$, have been investigated by small-angle neutron scattering (SANS) of annealed samples [4, 5]. The SANS curves show distinct interference maxima for all annealing time intervals, t_a, and temperatures, T_a. Figure 1 shows results for $T_a = 643$ K. In some (T_a, t_a) intervals the SANS curves obey the scaling law

$$f(x)|_{x=q/q_{max}} = I(q)/I(q_{max}) \tag{1}$$

(see figure 2) whereas they do not scale in other ones (see figure 3). In (1), $I(q)$ denotes the SANS intensity, q is the momentum transfer and q_{max} is the position of the maximum of the scattering intensity.

Spinodal decomposition [6] and hardcore-like distance correlations of decomposed regions [7, 8] have been proposed as possible explanations for the shape of the SANS curves. The analysis of the scattering behaviour [5] in terms of the linearized theory of spinodal decomposition [9] showed that spinodal processes might have some influence on the decomposition behaviour in the early stages. However, the observed shift of the position, q_{max}, of the maximum of the SANS curves and also the evolution of characteristic lengths of the observed fluctuations of the distribution of the scattering centres cannot be explained by the spinodal theory. Computer simulations [7, 8] based on hardcore arrangements of

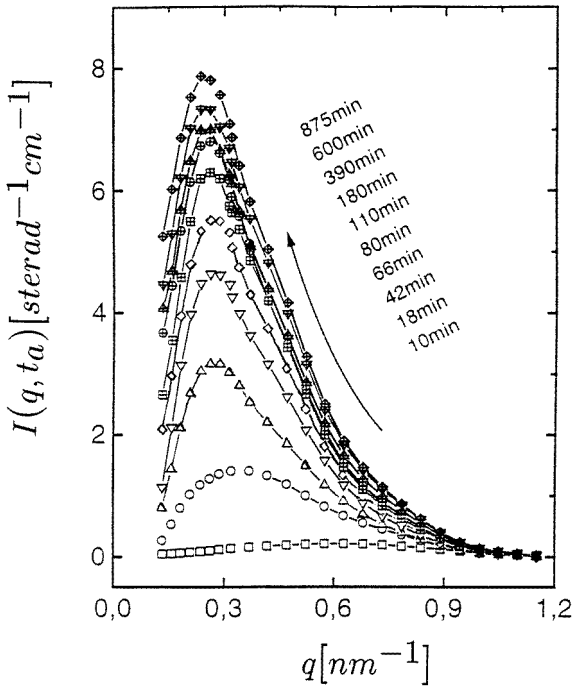

Figure 1. Experimental SANS curves obtained at $T_a = 643$ K for $t_a = 10$–875 min.

spherical precipitates reproduce the essential results of the SANS experiments [4, 5]. At small volume fractions ($c \approx 0.1$) and small radii of the precipitates (small as compared to the hardcore distance between the centres of the precipitates) there is, however, no plausible argument for the assumed hardcore interaction. Therefore, the computer model [7, 8] is reasonable for medium and high fractions of transformed volume but insufficient for low ones.

Here we propose an analytical model which includes nucleation and diffusion limited growth of precipitates. Hardcore repulsion of transformed regions is caused through interaction of depletion zones around the precipitates. The model can be treated analytically for volume fractions of precipitates below 0.125 only. For medium and high volume fraction it corresponds to the computer model as explained in [7, 8].

Experimental results [4, 5], especially the estimated Johnson–Mehl–Avrami exponent and the absence of a unique power law for the time evolution of the characteristic lengths, support the assumption that the decomposition is dominated by continuous nucleation and diffusion processes. During the early stages the volume fraction of transformed material is very small and one can start with the isolated-particle solution of the diffusion equation. Since the amorphous alloy is isotropic the solution for spherical symmetry of the precipitate is chosen (see, e.g. [10]). The exact solution for the concentration profile is well approximated by the function

$$\rho(r) = \begin{cases} \rho_m + (\rho_i - \rho_m)\exp[-a(r-R)] & r > R \\ \rho_p & r \leqslant R \end{cases} \tag{2}$$

where ρ_m, ρ_p, and ρ_i are the scattering length density in the matrix, in the precipitate, and at

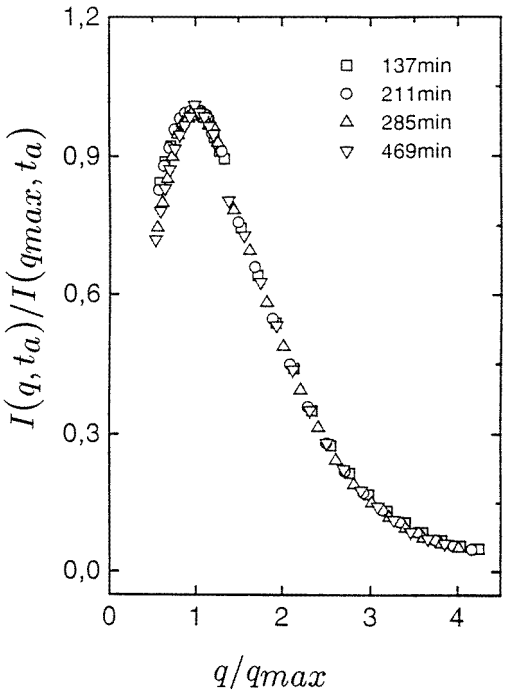

Figure 2. Rescaled experimental SANS curves according to (1); $T_a = 673$ K and different t_a (□ 137 min, ○ 211 min, △ 285 min, ▽ 469 min).

the interface, respectively. Comparison of (2) with the Laplace approximation for diffusion limited growth [10] yields

$$R = \sqrt{2\frac{\rho_m - \rho_i}{\rho_p - \rho_i}}\sqrt{Dt} \tag{3}$$

$$a = \alpha/R \tag{4}$$

where α is the order of 1 and depends on details of the diffusion process and on correlations between neighbouring precipitates. Parameter D characterizes the diffusion of possibly several types of atom resulting in the time evolution of the concentration profile, i.e. R and a in (2). In the early stage of decomposition ρ_m is constant and the condition $\frac{4}{3}\pi R^3(\rho_p - \rho_m) = 4\pi(\rho_m - \rho_i)\int_R^\infty r^2 \exp[-a(r-R)]\,\mathrm{d}r$ leading to

$$\frac{\rho_p - \rho_m}{\rho_m - \rho_i} = 3\frac{a^3R^3}{2 + 2aR + a^2R^2} \tag{5}$$

holds. For the considered multicomponent alloy the mean local scattering length density, $\rho(\boldsymbol{r})$, is given by

$$\rho(\boldsymbol{r}) = \sum_{n=1}^{5} c_n(\boldsymbol{r})b_n \tag{6}$$

where b_n is the scattering length of n-type atoms and $c_n(\boldsymbol{r})$ is their number density at position $\boldsymbol{r}$. (For the considered case of spherical particles the number of n-type atoms in volume element $\mathrm{d}V$ is $c_n(\boldsymbol{r})\,\mathrm{d}V = c_n(r)4\pi r^2\,\mathrm{d}r$.) Figure 4 shows the concentration profile

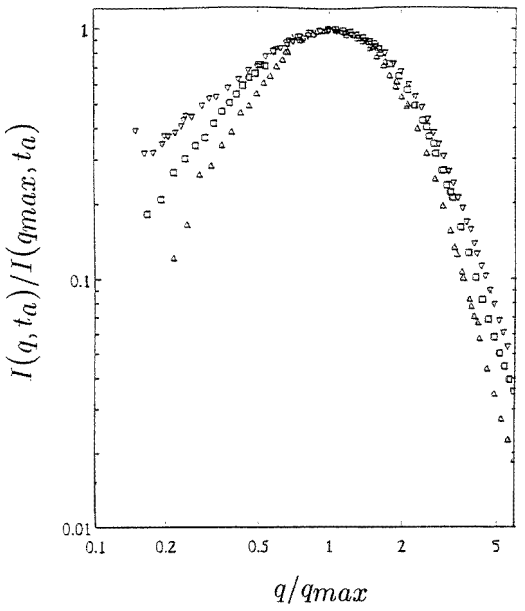

Figure 3. Rescaled experimental SANS curves at different T_a (▽ 623 K, □ 643 K, △ 660 K); $t_a \approx 600$ min).

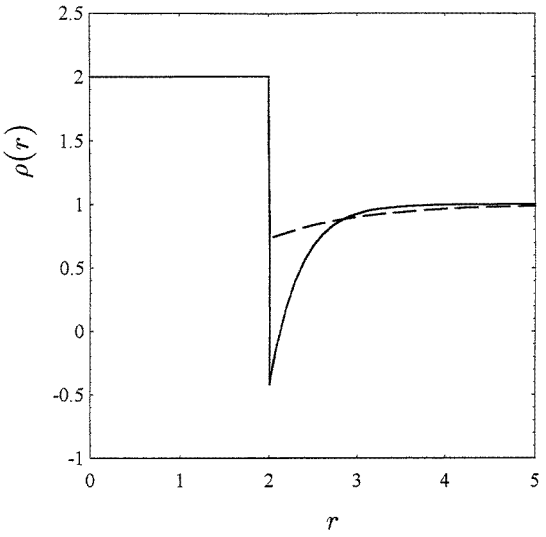

Figure 4. Mean local scattering length density, $\rho(r)$, for spherical precipitates with depletion zone; $\rho_p = 2$; $\rho_m = 1$, $R = 2$; dashed line: $\alpha = 1$; solid line: $\alpha = 3$.

(2) with a depletion zone around the precipitate of radius R for two different values of α and illustrates the meaning of the parameters.

The approximation (2) has the advantage that the corresponding scattering intensity is given explicitly (see [11] and references therein) by the expression

$$I_p(q) = \left[\frac{\rho_p - \rho_m}{\rho_m - \rho_i}\varphi(qR) - \phi(qR, aR)\right]^2 \tag{7}$$

where

$$\varphi(qR) = 3\frac{\sin(qR) - qR\cos(qR)}{(qR)^3} \tag{8}$$

and

$$\phi(qR, aR) = \frac{3}{qR[(qR)^2 + (aR)^2]}\left[\left(aR + \frac{(aR)^2 - (qR)^2}{(qR)^2 + (aR)^2}\right)\sin(qR) + \frac{2qaR^2}{(qR)^2 + (aR)^2}\cos(qR)\right]. \tag{9}$$

It should be noted that the scattering function (7) obeys exactly the scaling law (1) which was observed for wide ranges of (t_a, T_a) intervals (see figure 2).

The expression (7) for the small-angle scattering intensity and the corresponding relations (5, 8, 9) are valid for systems of non-interacting identical precipitates. This model would correspond to early stages of transformation processes initiated by instantaneous nucleation at random sites. In the present alloy the estimated value of the Johnson–Mehl–Avrami exponent [4, 5] suggests, however, continuous nucleation. Considering (3) and neglecting interactions of growing precipitates one obtains the corresponding particle size distribution

$$n(R) = \begin{cases} (2\mu/b^2)R & 0 < r \leqslant R_{max} \\ 0 & R > R_{max}. \end{cases} \tag{10}$$

The maximum radius of precipitates, $R_{max} = R(t_a)$, is given by (3) and $t = t_a$ where t_a is the annealing time, and μ is the constant nucleation rate.

The gradient of the concentration profile (2) is non-negligible within a sphere of radius of about $(R + 1/a)$. We interpret

$$R_{hc} = 2(R + 1/a) \tag{11}$$

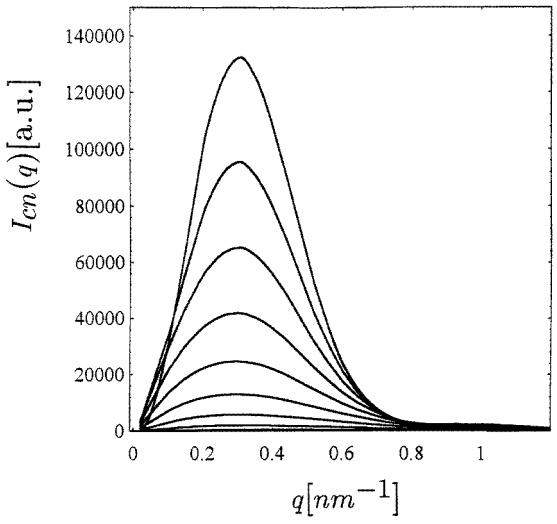

Figure 5. Small-angle scattering curves calculated from (14) and condition (5); $p_{hc} = 0.125$; $\alpha = 0.4$; $\rho_p = 2$; $\rho_m = 1$; $R_{max} = (6.3, 6.0, 5.7, 5.3, 4.9, 4.5, 4.0, 3.5)$ nm from top to bottom.

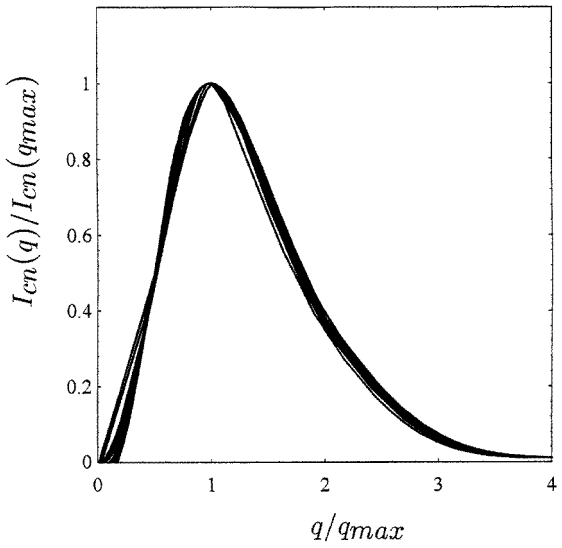

Figure 6. Rescaled theoretical SANS curves. Parameters are the same as in figure 5.

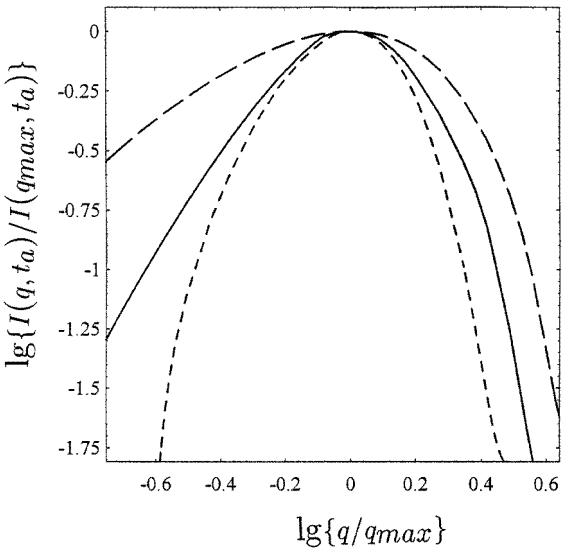

Figure 7. Rescaled theoretical SANS curves for different degrees of hardcore interaction, p_{hc}, and different depletion profiles, α. Dashed line: $p_{hc} = 0.03$, $\alpha = 0.4$; solid line: $p_{hc} = 0.125$, $\alpha = 0.4$; dotted line: $p_{hc} = 0.125$, $\alpha = 0.8$. The other parameters are the same as in figure 5.

as the minimum distance between the centres of two neighbouring precipitates and, correspondingly, as the hardcore distance used in the computer model [7, 8]. For small volume fraction, $c \leqslant 0.125$, the distribution of the centres of precipitates can be described by the Matérn hardcore model, and the corresponding scattering intensity is approximately

given [12] by

$$I_{hc}(q) = 1 - 8p_{hc}\varphi(qR_{hc}) \tag{12}$$

where φ is defined in (8) and p_{hc} is the packing fraction of the spheres in the Matérn model interacting by their hardcore diameter R_{hc}. (Parameter p_{hc} is also a measure for the degree of order of the arrangement of the interacting spheres.) The small-angle scattering intensity of a system of identical spherical precipitates, i.e. precipitates created by instantaneous nucleation, interacting through their diffusion zones is then given by

$$I_{in}(q) = I_p(q)I_{hc}(q). \tag{13}$$

If continuous nucleation occurs the precipitates obey the size distribution (10). Unfortunately, there is no analytical approach to the calculation of scattering intensities for hardcore systems with size distribution of radii except the solution for the correlation function of the very special Stienen model [14]. (This model is, however, not suitable for the present situation.) Therefore, we choose

$$I_{cn}(q) + \int_0^{R_{max}} (\tfrac{4}{3}\pi R^3)^2 n(R) I_p(q) I_{hc}(q)\,\mathrm{d}R \tag{14}$$

as an approximation for the small-angle scattering intensity. The approximation consists in that only the hardcore interaction of precipitates of the same size, i.e. the same nucleation time, is considered whereas correlations of precipitates of different size are neglected. (This approximation is reasonable for the considered low volume fractions. For detailed estimates see [13, 14].)

Figure 5 shows results for $I_{cn}(q)$ for a series of time steps, i.e. a series of R_{max} values. The shape of the curves and the shift of the maximum with increasing annealing time correspond to the behaviour of the experimental data presented in figure 1. Detailed analysis of expression (14) shows that the shift of the maximum towards lower q-values with increasing t_a is more pronounced for higher packing fraction, p_{hc}, of the interaction spheres. The width of the maximum and the skewness of the scattering curve are essentially governed by parameter α defined in (4) and also by p_{hc}.

The rescaled theoretical scattering curves are plotted in figure 6. Comparison with figure 2 shows that the agreement with the experimentally observed scaling behaviour is reasonable. Therefore, the following model for the decomposition mechanism can be suggested. Precipitates are formed through continuous nucleation and diffusion. Each precipitate has a constant scattering length density within a sphere of radius $R, 0 < R < R_{max}$, and is surrounded by a depletion zone. The radial dimension of the depletion zone is characterized by the quantity α^{-1}. The precipitates interact through their depletion zones which is described by a hardcore repulsion with a hardcore diameter of about $2R(1 + 1/\alpha)$. For the present alloy the values $\alpha \approx 0.4$ and $R_{max} = 4$ to 6 nm are typical.

The present model reproduces also the behaviour of the amorphous alloy in (T_a, t_a) intervals where the decomposition process does not obey the scaling law (1) (figure 3). The model suggests two possible reasons for this behaviour: variation of the degree, p_{hc}, of the hardcore interaction between precipitates of change of the parameter, α, of the depletion zone during annealing. Figure 7 shows rescaled theoretical curves for different values of p_{hc} and α. Since both parameters are, in a way, correlated (see equation (4)) experimental results of the type shown in figure 3 can be interpreted as consequences of changes of the diffusivity of atoms. This is plausible at least in cases where deviations of the scaling law (1) are related to differences of the annealing temperature (and corresponding changes of the diffusion constants). On the other hand, one may also expect deviations from (1) for constant T_a and long annealing time since annealing of metallic glasses may cause structural

relaxations and changes of the diffusion constants due to decreasing excess free volume. More detailed discussion of these effects requires additional experimental and theoretical work which is in progress.

References

[1] Inoue A, Zhang T and Masumoto T 1993 *J. Non-Cryst. Solids* **156–158** 473
[2] Inoue A, Zhang T and Masumoto T 1995 *Mater. Trans. JIM* **36** 391
[3] Peker A and Johnson W L 1993 *Appl. Phys. Lett.* **63** 2342
[4] Wiedenmann A, Keiderling U, Macht M-P and Wollenberger H 1996 *Mater. Sci. Forum* **225–227** 71
[5] Wiedenmann A 1997 *J. Appl. Crystallogr.* at press
[6] Schneider S 1997 *Frühjahrstagung des Arbeitskreises Festkörperphysik der DPG (Münster, 1997)*
[7] Uebele P and Hermann H 1996 *Modelling Simulation Mater. Sci. Eng.* **4** 203
[8] Uebele P, Wiedenmann A, Hermann H and Wetzig K 1997 *J. Appl. Crystallogr.* at press
[9] Cahn J W 1965 *J. Chem. Phys.* **42** 93
[10] Aaron H B, Fainstein D and Kotler G R 1970 *J. Appl. Phys.* **41** 4404
[11] Lembke U, Brückner R and Kranold W 1997 *J. Appl. Crystallogr.* at press
[12] Hermann H 1991 *Stochastic Models of Heterogeneous Material* (Zurich: Trans Tech) p 51
[13] Bertram W K 1996 *J. Appl. Crystallogr.* **29** 682
[14] Schlather M and Stoyan D 1997 *Advances in Theory and Applications of Random Sets* ed D Jeulin (Singapore: World Scientific) p 157